

sumption during variations in both synchronization of pulsatile support and LVAD uptake.

### Acknowledgments

This research was supported by NIH Grants No. HL29751, HL41777 and the Willem J. Kolff Development Fund. The authors thank S. Anglin, M. Brown Jr., P. Carlisle, D. Decker, A. Durtschi, M. Erickson, B. Hastings, G. Lamle, M. Painter, and P. Perkins for their valuable assistance.

### References

1. Baller D, Bretschneider HJ, Hellige G: A critical look at currently used indirect indices of myocardial oxygen consumption. *Basic Res Cardiol* 76: 163-181, 1981.
2. Vinten-Johansen J, Barnard RJ, Buckberg GD, Becker H, Duncan HW, Robertson JM: Left ventricular O<sub>2</sub> requirements of pressure and volume loading in the normal canine heart and inaccuracy of pressure-derived indices of O<sub>2</sub> demand. *Cardiovasc Res* 16: 439-447, 1982.
3. Pantalos GM, Marks JD, Riebman JB, et al: Left ventricular oxygen consumption and organ blood flow distribution during pulsatile ventricular assist. *ASAIO Trans* 34: 356-360, 1988.
4. Cohan G, Gewertz BL: Current research review: Measurement of myocardial oxygen consumption. *J Surg Res* 38: 305-313, 1985.
5. Kim YD, Nematzadeh D, Lees DE, et al: Halothane effects on subendocardial oxygen supply-demand balance: Estimation from intramyocardial tissue pressure and left ventricular pressure. *Anesth Analg* 64: 1149-1155, 1985.
6. Marzilli M, Sabbah HN, Stein PD: Supply-demand balance of subendocardial muscle: Estimation from intramyocardial pressure. *J Thorac Cardiovasc Surg* 79: 803-808, 1980.
7. Baird RJ: Myocardial tissue pressure. *J Thorac Cardiovasc Surg* 79: 809-811, 1980.
8. Kresh JY, Kerkhof PL, Goldman SM, Brockman SK: Heart-mechanical assist device interaction. *ASAIO Trans* 32: 437-443, 1986.
9. Baird RJ, Goldbach MM, de la Rocha A: Intramyocardial pressure: The persistence of its transmural gradient in the empty heart and its relationship to myocardial oxygen consumption. *J Thorac Cardiovasc Surg* 64: 635-646, 1972.

Vol. XXXV Trans Am Soc Artif Intern Organs 1989

## Computer Model of Ventricular Interaction During Left Ventricular Circulatory Support

JOHN C. WOODARD, DAVID J. FARRAR, EDNA CHOW, WILLIAM P. SANTAMORE,\*  
DANIEL BURKHOFF,† AND J. DONALD HILL

**The authors used a computer model of the heart and circulation to test the hypothesis that anatomic ventricular interactions are responsible for the observed instances of right ventricular failure during use of a left ventricular assist device. The model predicts that left ventricular pressure-unloading with a LVAD, in the presence of isolated systolic interaction, results in impairment of RV function, whereas with isolated diastolic interaction, RV function is improved. Due to competition between these two interactions, there is**

**a negligible overall effect of ventricular anatomic interactions in determining right ventricular function in the normal heart. *ASAIO Transactions* 1989; 35: 439-441.**

Use of left ventricular assist devices (LVADs) in patients with refractory cardiac failure has resulted in a significant incidence (~25%) of right ventricular (RV) failure.<sup>1</sup> One hypothesis for these episodes of RV failure is that large reductions in left ventricular (LV) pressure and volume during LV bypass significantly affect RV performance. The mechanism of this interaction is the shared ventricular septum and common muscle fibers in the free walls, which allow the volume and pressure in one ventricle to directly influence the volume and pressure in the other ventricle.<sup>2</sup> The postulated impairment of RV systolic performance with reduced LV pressure may, however, be counterbalanced by a beneficial diastolic effect due to the smaller LV volume and an increase in the RV diastolic compliance.<sup>1</sup> Thus, whether RV failure during LVAD use can be explained on the basis of ventricular interaction is not known.

To study the magnitude of these effects during LV pres-

From the Medical Research Institute and Department of Cardiovascular Surgery, Pacific Presbyterian Medical Center, San Francisco, California, \*Section of Cardiology, Wake Forest University Medical Center, Winston-Salem, North Carolina, and †Department of Medicine, Francis Scott Key Medical Centre, Baltimore, Maryland.

William P. Santamore's current affiliation is Philadelphia Heart Institute, Presbyterian Medical Center, Philadelphia, Pennsylvania.

Supported in part by grants 1-R01-HL-32202, 5-R01-HL-36365, and HL-36068 from the National Heart, Lung, and Blood Institute.

Reprint requests: David J. Farrar, PhD, Pacific Presbyterian Medical Center, 2351 Clay St, Room S637, San Francisco, CA 94115.

sure unloading with a LVAD, we used a computer model to isolate systolic and diastolic ventricular interactions and to predict their combined effects on RV function.

### Methods

The computer simulation of the heart is based on a time-varying elastance model that has been previously described.<sup>3</sup> Briefly, the model assumes a linear end-systolic pressure–volume relationship for each ventricle

$$P_{es} = E_{es}[V_{es} - V_0] \quad (1)$$

where  $P_{es}$  is the pressure at end systole,  $E_{es}$  is the maximal volume elastance,  $V_{es}$  is the end-systolic volume, and  $V_0$  is the volume at which ventricular pressure is zero. The diastolic pressure–volume relationship for each ventricle is described using an exponential function

$$P_{ed} = B[\exp(A(V_{ed} - V_0) - 1)] \quad (2)$$

where  $A$  and  $B$  are constants,  $P$  and  $V$  refer to pressure and volume, and the subscript  $ed$  indicates end-diastole. A time-dependent function  $e(t)$  describing the chamber stiffness between end-diastole and end-systole is used to combine these two equations so that

$$P[V(t), t] = e(t)\{P_{es}[V(t)] - P_{ed}[V(t)]\} + P_{ed}[V(t)] \quad (3)$$

Ventricular interaction occurring at end-systole is incorporated into the model using the method of Maughan,<sup>4</sup> in which the heart is divided into three functional units: the left and right ventricular free walls and the septal wall. Ventricular elastance for each ventricle is then made a function of both its free wall and the common septal wall acting in parallel. Diastolic interaction is modelled by making parameter  $A$  in equation 2 a linear function of the volume of the other ventricle, so that filling of one ventricle increases the pressure in the other chamber, and thus limits its end-diastolic volume.

**Figure 1** illustrates the electrical analogue used to simulate the cardiovascular system and LVAD. The two ventricular free walls and the ventricular septum are shown as time-varying elastances (capacitors), which are governed by equation 3. Anatomic valves between the ventricles and atria and arteries are represented by diodes. The simulated LVAD is also shown as a time-varying elastance ( $E_{vad}$ ) connected to the left ventricle by a diode (representing the inflow valve in the physical LVAD) and a filling resistance ( $R_f$ ). Ejection of blood from the LVAD proceeds via an out-flow valve and an ejection resistance ( $R_e$ ) into the systemic arteries.

In the clinical setting, LVAD filling and ejection is controlled by a pneumatic drive console that alternately supplies vacuum and pressure to a rigid case enclosing a deformable blood sac.<sup>5</sup> This is modelled by changing the elastance of the sac over a wide range. During the simulated LVAD filling phase,  $E_{vad}$  is made effectively zero, corresponding to the very low elastance of the collapsed LVAD sac enclosed in a partial vacuum. Despite the low elastance, the rate of venous return and volume of the LVAD sac are such that complete LVAD filling does not occur during

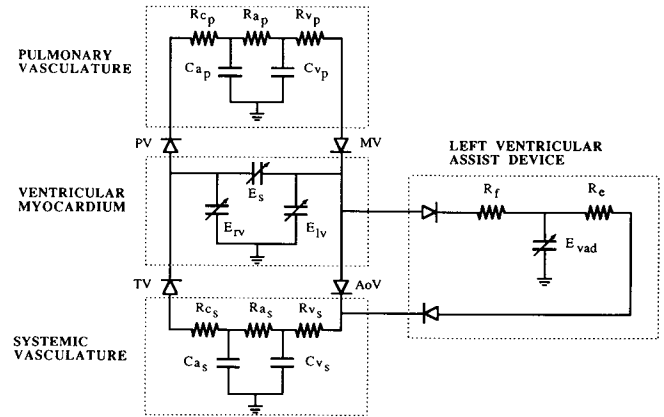


**Figure 1.** Schematic diagram of the electrical analogue used to simulate the cardiovascular system and the LVAD. The heart is composed of three time-varying capacitors representing elastances  $E_{rv}$  (elastance of the right free wall),  $E_{lv}$  (elastance of the left free wall), and  $E_s$  (elastance of the septum). The LVAD is also shown as a time-varying elastance ( $E_{vad}$ ) connected to the circulation by its filling and ejecting resistances ( $R_f$  and  $R_e$ ). Diodes represent the prosthetic valves of the LVAD and the aortic, pulmonary, mitral, and tricuspid valves (AoV, PV, MV, and TV respectively). The systemic and pulmonary vasculature are shown as a network of resistors (corresponding to hydraulic resistance) and capacitors (representing compliance). Uppermost subscripts  $v$  and  $a$  indicate venous and arterial components respectively, while lower subscripts  $s$  and  $p$  refer to whether these components are part of the systemic or pulmonary vasculature. The characteristic impedance of the systemic and pulmonary arterial systems are shown as  $R_{cs}$  and  $R_{cp}$ .

steady-state conditions. Ejection of blood from the simulated LVAD is accomplished by increasing  $E_{vad}$  so that the pressure developed is constant at  $\sim 180$  mmHg, until the volume of blood in the device falls to zero. Thus, LVAD ejection occurs at a rate determined by the difference between this drive pressure and that in the systemic arteries. The LVAD operates in counterpulsation so that filling occurs during LV systole and ejection proceeds during ventricular diastole.

Systemic and pulmonary vasculature are simulated using an electrical analogue of a 4 element "windkessel." The contractile properties of the atria are not modelled, but are embraced in the venous parameters. Values for the vascular and ventricular parameters (including the interaction variables) are assigned as per a previous report,<sup>3</sup> and represent typical values for a 20 kg dog.

### Protocol

Control runs were produced by running the simulation with the stroke volume determined by the model parameters. The LVAD was then used to pressure unload the LV by setting the LVAD stroke volume to that of the control runs. To produce a range of right ventricular end-diastolic volumes, the computer simulation is volume loaded or exsanguinated by addition or removal of blood from the systemic venous volume. Following each volume change, the right ventricular stroke work (RVSW) is calculated from the area inside the pressure–volume ( $P$ - $V$ ) loop. Simulations were run

under conditions of isolated systolic interaction, isolated diastolic interaction, and a combination of the two.

## Results

The model predicts that complete LV pressure unloading with the LVAD during isolated systolic interaction produces a reduction in effective right ventricular systolic elastance, which in turn causes the P-V loop to shift to the right, and peak RV pressure to be reduced (Figure 2, first panel). With isolated diastolic interaction, the model also predicts a rightward shift during LVAD, due to the increase in RV diastolic compliance but with an increase in peak RV pressure. When both interactions are enabled, representing the model predictions for the normal canine heart, no significant changes in RV peak pressure or stroke work are seen, and the LVAD results only in a shift of the P-V loop to larger volumes.

Without any ventricular interactions, the model predicts no influence of LV unloading on the right ventricular function curve. RVSW, however, is impaired during LVAD in the presence of isolated systolic interaction (first panel of Figure 3) and enhanced in the presence of isolated diastolic interaction (second panel of Figure 3). When both interactions are operative, the model predicts that these effects will counteract each other, with a resultant parallel shift to larger end-diastolic volumes, but with no change in slope at physiologic volumes.

## Discussion

The model specifies that one ventricle's pressure development is a function of its own volume and elastance, as well as the end-systolic pressure in the contralateral ventricle. Therefore, the reduction in LV end-systolic pressure to near zero during LVAD unloading reduces the pressure generating capacity of the right ventricle. This is equivalent to a reduction in the slope of the end-systolic P-V relationship and, thus, a reduction in the RV effective contractility. Pressure and stroke work developed by the RV for a given end-diastolic volume is therefore predicted to be reduced with systolic interactions.

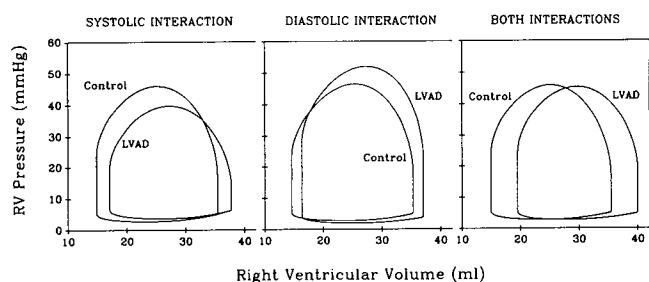


**Figure 2.** Pressure-volume diagrams of the right ventricle prior to (control) and during complete LV pressure-unloading with the LVAD. The effects of systolic and diastolic interaction are shown individually in the first two panels with the combined effect shown in the third panel.

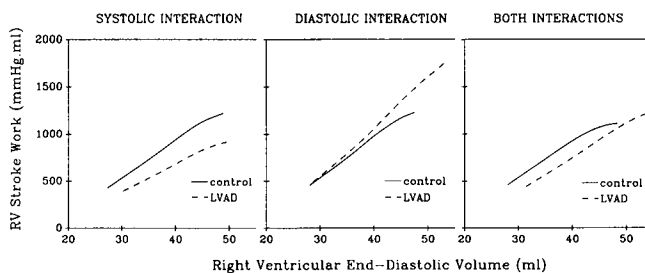


**Figure 3.** Right ventricular stroke work (RVSW) as a function of RV end-diastolic volume without LV unloading (control) and with the LV completely pressure unloaded with the LVAD. Over the range of volumes and pressures studied, the model predicts that RVSW is enhanced with the LVAD by diastolic interaction and impaired by systolic interaction. With both interactions, the ventricular function curve is shifted to the right, but with an unchanged slope.

Diastolic interactions also cause a rightward shift in the RV pressure volume loop, but in this case due to increased RV compliance resulting from a reduced LV volume. The combination of a larger end-diastolic volume and unaltered end-systolic P-V relationship dictates a larger developed pressure and stroke work.

It is apparent from Figure 3 that both the diastolic and systolic ventricular interactions would be significant in isolation. However, as a result of their competing influences, the model predicts that overall RV function in the normal heart is not significantly altered due to LV unloading. Although the P-V curve is shifted to the right, the slope of the ventricular function curve is unchanged, resulting in an unimpaired ability to increase RV stroke work with increasing preload. In the current analysis, we have only addressed the normal heart and have not studied the role of the ventricular interactions under various pathophysiologic conditions. The results of this simulation, however, are in agreement with our experimental results of right ventricular dimension-pressure relationships in normal pigs during graded LV unloading with a LVAD.<sup>6,7</sup>

## References

1. Farrar DG, Compton PG, Hershon JJ, Fonger JD, Hill JD: Right heart interaction with the mechanically assisted left heart. *World J Surg* 9: 89-102, 1985.
2. Bove AF, Santamore WP: Ventricular interdependence. *Prog Cardiovasc Dis* 23: 365-388, 1981.
3. Santamore WP, Burkhoff D: Haemodynamic consequences of ventricular interaction as assessed by model analysis. In review.
4. Maughan WL, Sunagawa K, Sagawa K: Ventricular systolic interdependence: Volume elastance model in isolated canine hearts. *Am J Physiol* 253: H1381-1389, 1987.
5. Farrar DJ, Compton PG, Lawson JH, Hershon JJ, Hill JD: Control modes of a clinical ventricular assist device. *IEEE Eng Med Biol* 5: 19-25, 1986.
6. Farrar DJ, Compton PG, Verderber A, Hill JD: Right ventricular end-systolic pressure-dimension relationship during left ventricular bypass in anesthetized pigs. *ASAIO Trans* 32: 278-281, 1986.
7. Chow E, Farrar DJ: Effects of graded left ventricular pressure reductions on systolic right ventricular performance. *Am J Physiol Heart Circulatory Physiol* (in press).